Catalysis Letters Vol. 100, Nos. 3–4, April 2005 (© 2005)
DOI: 10.1007/s10562-004-3452-7

N-alkylation of aniline with ethanol over an industrial niobic acid catalyst – influence of water formation on kinetics and selectivity

B. Frank[a], D. Habel[b] and R. Schomäcker[a]

[a]*Institute of Chemistry, Technical University of Berlin, Straße des 17. Juni 124, Berlin, D-10623 Germany*
[b]*Institute of Material Sciences and Technologies, Technical University Berlin, Englische Straße 20, Berlin, D-10587 Germany*

Received 15 November 2004; accepted 24 November 2004

The reaction of aniline with ethanol was carried out over an industrial niobic acid catalyst in a fixed bed reactor at atmospheric pressure and 220–260 °C. The main products, *N*-ethylaniline and *N*,*N*-diethylaniline were formed consecutively. A kinetic study including a model discrimination between several Hougen/Watson type rate equations led to an Eley/Rideal mechanism, where the reaction of gas phase aniline with adsorbed ethanol is the rate determining step. As second adsorbing agent, water inhibits the reaction in higher partial pressures. *N*-alkylation was the main reaction observed but the addition of water decreased the selectivity and up to 15% *C*-alkylated products were found. The apparent activation energies for the first and second *N*-ethylation are 85.6 and 70.7 kJ/mol, respectively. The high equilibrium constants indicate a nearly irreversible reaction.

KEY WORDS: alkylation; ethylation; aniline; niobic acid; Eley/Rideal; Hougen/Watson

1. Introduction

Alkylanilines are important intermediates for the production of dyes, herbicides or pharmaceuticals. Solid acid catalysts like niobic acid (hydrated niobium pentoxide $Nb_2O_5{\cdot}nH_2O$) have been applied to gas phase alkylation of aniline with several alcohols for about 10 years [1]. Heterogenous solid–gas catalysis is a clean, environmentally safe method and the catalysts are easier to handle than those in previous processes using mineral acids. A literature survey on aniline alkylation indicated that considerable attention has been focused on the synthesis of new catalysts such as metal oxides [2–5], mixed oxides of the spinel type [6–8], phosphates [2,9, 10], clays [4,11] and zeolites [4,12,13]. Most of them show high activity for aniline alkylation and even a high selectivity to *N*-alkylanilines against toluidines. In addition, niobic acid shows a good resistance against water vapor and in spite of its water content keeps a high acid strength of $H_0 = -5.6$, which is corresponding to 70% H_2SO_4 [14–17]. That makes niobic acid a suitable solid acid catalyst with an excellent long term stability, for reactions with water as a reactant or a by-product like hydration/dehydration, esterification/ hydrolysis or condensation reactions [17–19]. Moreover, the acidic property of niobic acid can be increased by treatment with sulfuric or phosphoric acid [19–21]. On the contrary to other metal oxides, niobic acid looses catalytic activity by heat treatment above 400–500 °C [14,15,22] due to an irreversible dehydration and the formation of crystalline niobium pentoxide Nb_2O_5 [22], which shows no surface acidity (table 1).

In previous kinetic analysis selective *N*-alkylation of aniline was found to be a consecutive reaction to *N*-alkylaniline and *N*,*N*-dialkylaniline [1,3]. For aniline alkylation with methanol over MgO and Al_2O_3 solid acid catalysts, the following reaction scheme was proposed (figure 1) [3,23]. After adsorption of methanol and aniline on the solid acid surface, the rate determining step was suggested to be the attack of methyl cation to anilino group (step III).

A more detailed reaction mechanism has been proposed by Narayanan and Deshpande [4,5], who made a difference between Brønsted and Lewis acid sites. They found that Brønsted acid sites mainly catalyze *N*-alkylation as well as neighboring Brønsted and Lewis acid sites. Lewis acid sites were suggested to catalyze only *C*-alkylation of aniline. An investigation on aniline methylation over zeolite resulted in the proposal of a similar reaction mechanism [24]. The influence of the acid strength on the regioselectivity of aniline methylation has been investigated by several authors [2,25,26]. They suggested that strong, medium and weak acid sites produce *C*-alkylate and coke, *N*,*N*-dimethylaniline and *N*-methyltoluidine, and *N*-methylaniline, respectively. Niobic acid, due to its weak acidity and high water content, seems to be an ideal catalyst for *N*-alkylation of aniline.

2. Experimental

2.1. Catalyst and materials

An industrial niobic acid catalyst was used for a kinetic investigation. Manufacturing of the catalyst is described in the patent specification [27]. The catalyst is produced by H.C. Starck and applied e.g., by Bayer for

Table 1
Symbols and indices used in this work

Symbols		
k	[s^{-1}]	Rate constant
K	[bar^{-1}]	Adsorption equilibrium constant
K		Reaction equilibrium constant
p	[bar]	Partial pressure
r	[bar/s]	Reaction rate
T	[°C]	Reaction temperature
Indices		
1		Monoethylation
2		Consecutive diethylation
A		Aniline
M		*N*-Ethylaniline
D		*N*,*N*-Diethylaniline
E		Ethanol
W		Water

the studied reaction. The 5 × 5 mm cylindrical pellets, containing graphite as inert additive, were crushed and sieved to a defined particle size (20–25 Mesh) in order to reduce inner particle diffusion limitation. The BET surface area, the pore volume and the average pore diameter were determined by nitrogen adsorption using a Micromeritics Gemini 2375 apparatus after evacuating the sample at 200 °C for 2 h. The water content was determined by weight loss after high temperature treatment of the catalyst powder. The adsorbed water was removed by evacuation at 200 °C. In order to obtain a water-free ceramic substance, the powder was afterwards calcined at 1000 °C for 12 h. The carbon content was quantified by carrier gas hot extraction using a Horiba EMIA 320 V instrument. The results are listed in table 2. The surface area determined complies well with those measured by Tanabe [16], who found 164, 126 and 42 m^2/g after evacuation at 100, 300 and 500 °C, respectively.

Amorphous niobic acid was found to have the composition $H_8Nb_6O_{19}{\cdot}nH_2O$ with n = 0, 3, 6, 12 or 18, depending on the temperature of pretreatment [1]. An elemental analysis of the catalyst showed that the catalyst contained no other additive but carbon so the composition of this catalyst can be written as $H_8Nb_6O_9{\cdot}5.05H_2O$. This indicates, that the hydration of the material is not homogeneous. Structural data from XRD could not be obtained because of the amorphous modification. The structure of crystalline niobic acid is given by Chernyshkova [17].

All the materials used in this work were of high purity (99.5 + %). Distilled water and ethanol were degassed at 200 mbar, the other substances were used without further purification.

2.2. Reaction procedure

All the kinetic measurements were performed in the gas phase under atmospheric pressure. The liquid reactants were mixed and pumped into a vaporizer by a HPLC pump (Dionex P 580A LPG). The well-thermostated gas mixture was introduced into a stainless steel tubular reactor (10 mm ID) with the catalyst bed stabilized between two layers of inert pyrex beads. A Fe–Co thermocouple was placed in the middle of this catalyst bed to adjust the temperature. The reactor was heated by a surrounding aluminium block containing six heating cartridges. For each reaction, a catalyst mass of 1.0 g (1.2 ml) was used. The condensed reaction product mixture was analyzed by GC (Siemens SiCHROMAT 3) with TCD using a 30 m × 0.25 mm Rtx-5MS column (5% diphenyl–95% dimethyl polysiloxane). For peak identification and quantification, a calibration was made by using pure samples of the expected products.

For kinetic modeling, the reactor was fed with different combinations and molar ratios of the reactants. The reaction temperature was varied between 220 and 260 °C. In addition to both the forward and backward reactions, the influence of water vapor on the catalytic activity was investigated.

3. Results and discussion

3.1. Kinetic model

After GC analysis of the condensed product gas mixture, the partial pressures of the components could be calculated by the peak areas of aniline, *N*-ethylaniline and *N*,*N*-diethylaniline followed by the material balances. By-products as toluidines and diethylether were not observed or in negligible quantities for kinetic modeling (<1%), except for the experiments on the influence of water vapor where toluidines were indenti-

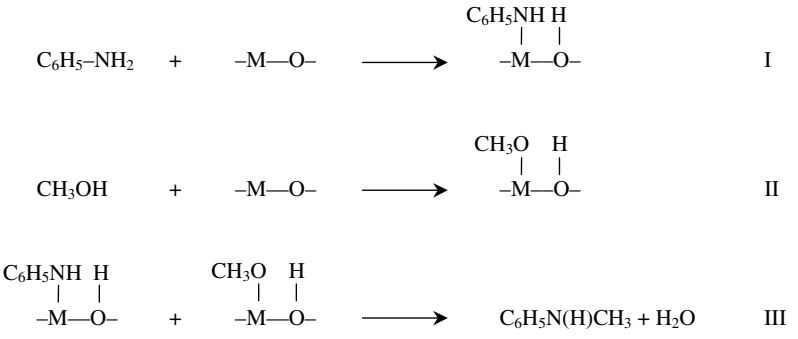

Figure 1. Proposed reaction scheme for aniline methylation over metal oxide catalysts [3,23].

Table 2
Properties of the industrial niobic acid catalyst

BET surface area	139 m^2/g
Pore volume	0.16 cm^3/g
Average pore diameter	5.07 nm
Water (loss up to 200 °C)	11.0%
Water (loss up to 1000 °C)	16.4%
Carbon content	3.4%

fied up to 15%, which may affect the kinetic constants in the same order of magnitude. The observed reaction scheme was that of an consecutive *N*-alkylation.

$$\mathrm{PhNH_2 + EtOH} \underset{K_1}{\overset{r_1}{\rightleftharpoons}} \mathrm{PhN(H)Et + H_2O}$$

$$\mathrm{PhN(H)Et + EtOH} \underset{K_2}{\overset{r_2}{\rightleftharpoons}} \mathrm{PhNEt_2 + H_2O}$$

For the kinetic model, two Eley/Rideal type rate equations of the Hougen/Watson formalism (1) were chosen by model discrimination. These equations were used for the curve simulation in all the diagrams (figures 2, 3, 5 and 7). The symbols and indices are listed in table 1.

$$r_1 = \frac{k_1 K_E (p_E p_A - p_W p_M / K_1)}{1 + K_E p_E + K_W p_W}$$
$$r_2 = \frac{k_2 K_E (p_E p_M - p_W p_D / K_2)}{1 + K_E p_E + K_W p_W} \quad (1)$$

More simple Eley–Rideal type rate expressions (2) were not suitable to fit the kinetic data because of the water inhibition, especially at higher conversions.

$$r_1 = k \frac{K_E p_E}{1 + K_E p_E} p_A \quad (2)$$

For the determination of the kinetic parameters, the initial reaction rate was measured at different temperatures and for a wide range of molar ratios. In the forward reactions the aniline and *N*-ethylaniline conversions were kept between 5 and 15% whereas in the backward reactions *N*-ethylaniline and *N*,*N*-diethylaniline conversions above 3% could not be observed. For the forward reaction, the flow rate of the liquid mixture was 0.3, 1.0 and 3.0 ml/min and 0.03, 0.1 and 0.3 ml/min for the backward reaction at 220, 240 and 260 °C, respectively.

Figure 2 shows the initial reaction rate of *N*-ethylaniline formation versus the molar fraction of ethanol in a binary ethanol/aniline mixture at T = 240 °C. It can be clearly seen that the maximum rate is shifted to an excess of aniline, indicating an influence of ethanol adsorption on the overall reaction rate. The same behavior was observed for in the reaction rate of *N*,*N*-diethylaniline formation versus the molar fraction of ethanol in a binary ethanol/*N*-ethylaniline mixture at all temperatures, shown at T = 240 °C (also depicted in figure 2). Those datasets were used to determine both reaction rate constants k_1, k_2 and the adsorption constant of ethanol K_E for the temperatures 220, 240 and 260 °C.

The backward reactions and water inhibition were negligible because of the low partial pressures of water, *N*-ethylaniline and *N*,*N*-diethylaniline, respectively. The effect of water adsorption was investigated by the addition of water to the reaction mixture. Figure 3 shows the reduced reaction rate versus the molar fraction of ethanol in a ternary ethanol/aniline/water mixture, where the ethanol/aniline molar ratio was kept constant at 0.5, 1 and 2 at T = 240 °C, respectively. The trajectories taken in these experiments are sketched

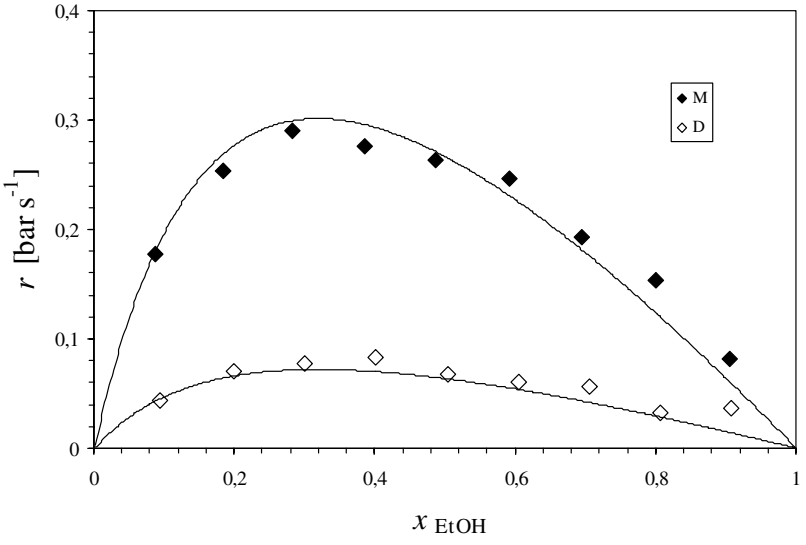

Figure 2. Initial reaction rates for *N*-ethylation of aniline (M) and *N*-ethylation of *N*-ethylaniline (D) as a function of the molar fraction of ethanol in the binary reaction mixture. Catalyst: niobic acid, T = 240 °C.

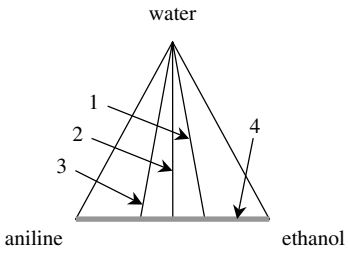

Figure 3. Initial reaction rates for *N*-ethylation of aniline as a function of the molar fraction of ethanol. The ethanol/aniline molar ratio is kept constant at 0.5, 1 and 2, respectively and the water partial pressure was varied. Catalyst: niobic acid, $T = 240$ °C. The dashed lines show the fit for a kinetic model (Eley–Rideal) neglecting water adsorption whereas the grey line indicates the reaction rate without water inhibition.

in the 3-component mixture diagram in figure 4. Again, the backward reaction could be neglected because of the low partial pressure of *N*-ethylaniline. These datasets were used to determine the water adsorption constant K_W. In contrast, the optimum fits ignoring the influence of water are also shown as dashed curves.

In order to obtain the equilibrium constants, the backward reactions were investigated. Figure 5 shows the backward reaction rate versus the molar fraction of water in a binary water/*N*-ethylaniline and water/*N*,*N*-diethylaniline mixture. The very low conversions caused a relatively low accuracy of measurement, so the influence of water adsorption on the backward rate could not be confirmed. The Eley/Rideal model was adapted from the forward reaction and only the backward reaction rate constants and the equilibrium constants for both reactions were fitted.

The results of all the fits are listed in table 3, of which the activation energies, reaction enthalpies and adsorption enthalpies were obtained from an Arrhenius plot (figure 6). Those data are assembled in table 4.

The apparent activation energies of the alkylation reactions are a little higher than those determined for γ-alumina by Ko *et al.* (62.7 and 48.3 kJ/mol, respectively) [3]. The reduction of the activation energy of the second alkylation can be explained by the electron-donating effect of the alkyl group, which accelerates the second alkylation. Both ethylations are slightly exothermic reactions, which is also confirmed by literature data. The reaction enthalpies for amine alkylation with alcohols calculated with medium binding energies of O–C, O–H, N–C and N–H bonds range from ± 0.0 to -26 kJ/mol [28,29]. The dependency of the equilibrium constant on temperature can be described by the van't Hoff equation, which confirms the reliability of the obtained data for the reaction enthalpy.

In order to verify the kinetic model obtained by the differential method longer contact times were simulated including all the kinetic data and it was found that this model can predict the reaction up to equilibrium very well. Figure 7 shows the comparison between the calculated and experimental data for an ethanol/aniline molar ratio of 4:1 at $T = 240$ °C. There was only a very little deviation from the experimental data, which could be reduced by varying the kinetic constants by <5%. It is clearly seen that *N*,*N*-diethylaniline formation follows an S-shaped curve while the concentration of *N*-ethylaniline runs through a maximum indicating that the second ethylation occurs consecutively.

The resulting kinetic model is an Eley–Rideal model indicating that the adsorption of ethanol has major influence on the overall reaction rate. Aniline either adsorbs very fast or reacts directly from the gas phase with adsorbed ethanol. Water vapor slows down the reaction not because of a possible backward reaction but due to an inhibiting effect as a strong adsorbent on the niobic acid surface. Based on these kinetic data and considering previous reports on the mechanism [4,24],

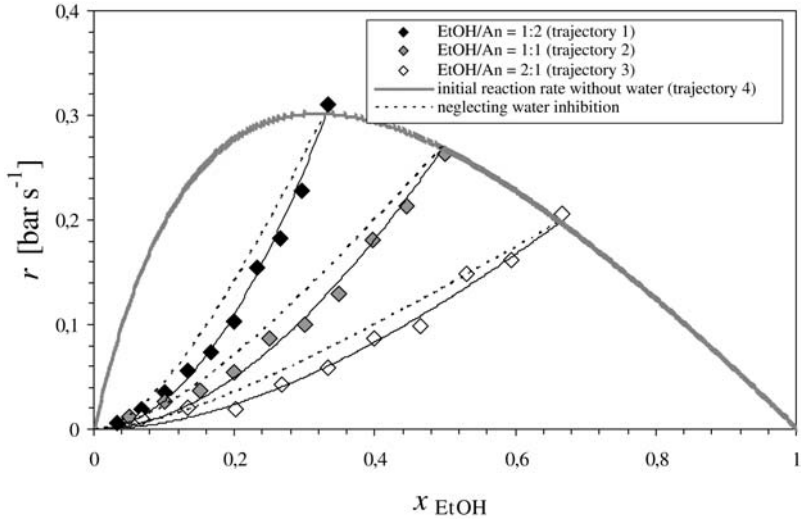

Figure 4. Three-component mixture diagram of the ternery aniline/ethanol/water mixture showing the trajectories of the feed composition when investigating the influence of water vapor on the reaction rate.

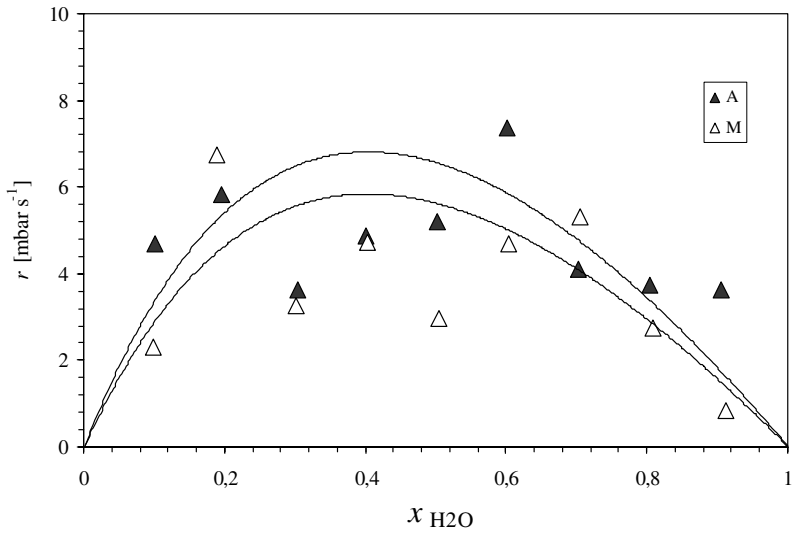

Figure 5. Initial reaction rates for *N*-ethylaniline (A) hydrolysis and *N*,*N*-diethylaniline (M) hydrolysis as a function of the molar fraction of water in the binary reaction mixture. Catalyst: niobic acid, $T = 240$ °C.

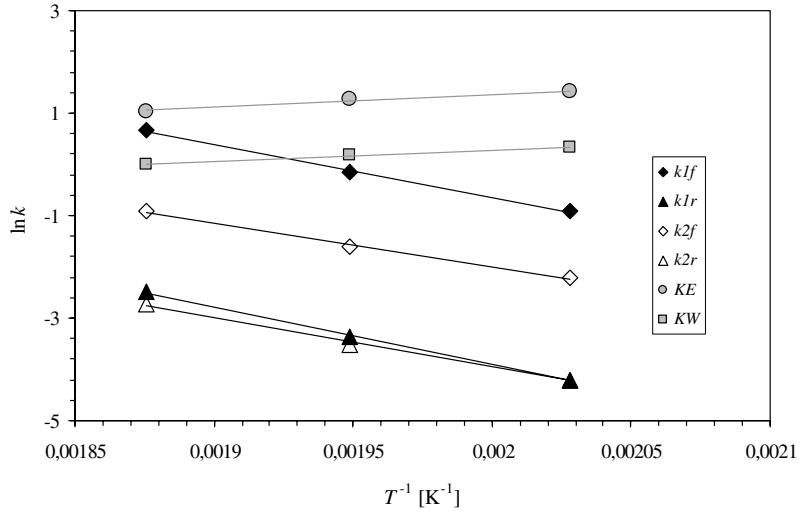

Figure 6. Arrhenius-plot of the rate constants and the adsorption equilibrium constants for aniline ethylation over niobic acid.

the following reaction mechanism for aniline ethylation is suggested (figure 8).

Selective *N*-ethylation of aniline is supposed to take place on Brønsted acid sites because crystalline and water-free Nb_2O_5 was found to be inactive as alkylation catalyst. Pre-adsorption of ethanol and formation of surface ethoxy groups are in agreement with the kinetic model as well as aniline reacting out of the gas phase. The six-membered transition state was adapted by

Table 3
Experimental results of reaction rate constants and adsorption constants for aniline ethylation as a function of temperature

T [°C]	k_1 [s^{-1}]	k_2 [s^{-1}]	K_1	K_2	K_E [bar^{-1}]	K_W [bar^{-1}]
220	0.40	0.11	26.7	7.3	4.1	1.4
240	0.85	0.20	24.2	6.7	3.6	1.2
260	1.92	0.40	23.2	6.2	2.8	1.0

Table 4
Experimental results of activation energies, reaction enthalpies and adsorption enthalpies for ethylation of aniline

	First ethylation	Second ethylation
E_A [kJ/mol]	85.6	70.7
$\Delta_R H$ [kJ/mol]	−7.6	−9.3
$\Delta_{ads}H_E$ [kJ/mol]	−21.3	
$\Delta_{ads}H_W$ [kJ/mol]	−18.0	

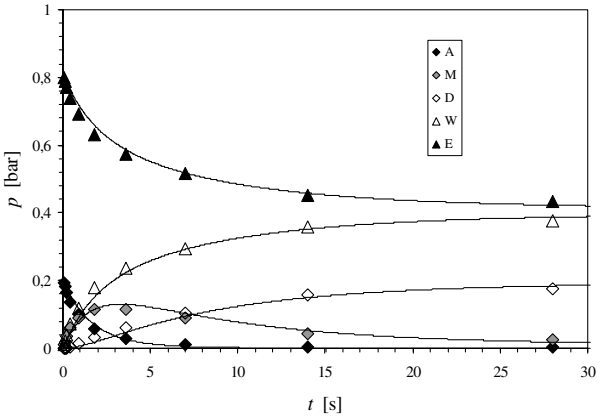

Figure 7. Calculated partial pressures of aniline (A), *N*-ethylaniline (M), *N*,*N*-diethylaniline (D), ethanol (E) and water (W) in comparison with experimental data. Aniline/ethanol molar ratio 4:1, catalyst: niobic acid, $T = 240$ °C.

mechanistic investigations on aniline methylation on a Brønsted acid zeolite catalyst by Ivanova *et al.* [24]. They suggest that the second reaction step, the attack of the aniline molecule on the surface methoxy group, to be very fast. So the formation of surface methoxy groups is the rate determining step of the overall reaction. In our case, we found the reaction step, which is the attack of aniline out of the gas phase on the pre-adsorbed ethanol molecule, to be the rate determining one. This change in the kinetic description of the reaction may have its reason in two differences between our and Ivanova's experiments. First, amorphous solid acid catalysts and zeolites have completely different pore structures which have influence on the material transport. Second, the alkylation was carried out with ethanol in stead of methanol. It is possible that the more bulky ethyl group makes the aniline attack more difficult so this reaction step becomes rate determining. However, the reaction mechanism is much more difficult than shown in the simplified scheme depicted in figure 1.

Because of a similar dependence of the reaction rate on the ethanol partial pressure, this reaction scheme is also proposed for the consecutive *N*-ethylation of *N*-ethylaniline. The lower reaction rate constant k_2 versus k_1 can be explained with a steric hindrance, though *N*-ethylaniline should be more reactive due to an electron donating effect of its ethyl group at the nitrogen atom [3]. The measured data could not prove a water adsorption effect on the backward reaction kinetics because this effect was within the range of experimental error. By supposing that the same reaction pathway applies and again the surface ethoxy group formation is the rate determining step, a similar Eley–Rideal mechanism was used for the kinetic fit.

Water vapor in the reaction mixture results in a reduced catalytic activity of the niobic acid catalyst due to the adsorption of water molecules on the surface. Of course, the surface acidity on the top of this layered structure is much weaker that the Brønsted acidity of dry niobic acid and the reaction mechanism may change because the formation of a surface alkoxy group will become more difficult on adsorbed water molecules.

3.2. Selectivity

In most of the experiments with a binary ethanol/aniline or ethanol/*N*-ethylaniline feed there was a formation of >99.5% *N*-alkylated product against *C*-alkylation. An influence of the reaction temperature was not observed in the chosen small temperature interval from 220 to 260 °C. Also the ethanol/aniline molar ratio was found to have no effect on the *C*-alkylation. Surprisingly, the selectivity decreased by adding water to the reaction mixture. The selectivity of *N*-alkylation towards *C*-alkylation as a function of the water partial pressure for $T = 240$ °C is depicted in figure 9.

Up to now, this experimental result can not be explained but it was highly reproducible. The selectivity is expected to increase in the opposite way. Water adsorption on the niobic acid surface was expected to result in the formation of weaker Brønsted acid sites, which normally catalyze *N*-alkylation much more than *C*-alkylation. A similar behavior was observed in the

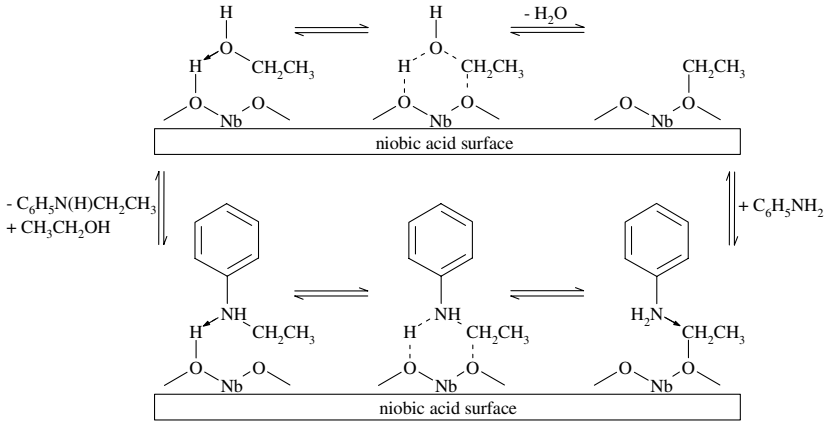

Figure 8. The proposed reaction mechanism of *N*-ethylation of aniline on niobic acid.

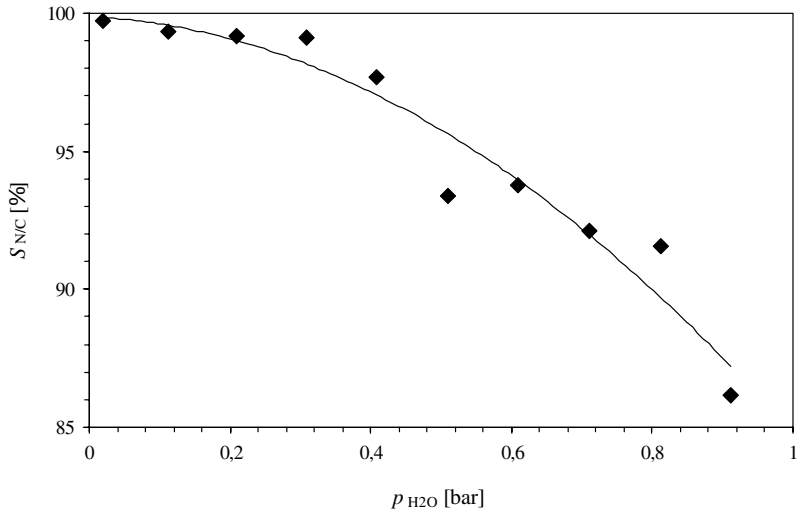

Figure 9. Selectivity of *N*-alkylation versus *C*-alkylation as a function of the partial pressure of water in the reaction mixture. Catalyst: niobic acid, $T = 240$ °C.

integral curves (figure 7). After an initial selectivity of 99.5% at 5% aniline conversion and a low water partial pressure, the selectivity decreases to 92% overall selectivity at full aniline conversion.

4. Conclusions

An industrial niobic acid catalyst was used for kinetic investigations on the gas phase *N*-ethylation of aniline with ethanol in the temperature range of 220 to 260 °C. The nearly irreversible consecutive *N*-ethylation can be described by an Eley–Rideal mechanism where water as inhibiting agent reduces the overall reaction rate. The apparent activation energies of the first and second ethylation are 85.6 and 70.7 kJ /mol, respectively. The selectivity of *N*-alkylation versus *C*-alkylation was high under water-free reaction conditions but decreased to 85% in the presence of water.

References

[1] O. Immel, R. Schomäcker, C. Fröhlich, V. Glock and H. Waldmann, Chem. Ing. Tech. 66 (1994) 8.
[2] F.M. Bautista, J.M. Campelo, A. Garcia, D. Duna, J.M. Marinas and A.A. Romero, Appl. Catal. A 166 (1998) 39.
[3] A.N. Ko, C.L. Yang, W. Zhu and H. Lin, Appl. Catal. A 134 (1996) 53.
[4] S. Narayanan and K. Deshpande, Appl. Catal. A 199 (2000) 1.
[5] S. Narayanan and K. Deshpande, J. Mol. Catal. 104 (1995) L109.
[6] K. Sreekumar, T. Mathew, S.P. Mirajkar, S. Sugunan and B.S. Rao, Appl. Catal. A 201 (2000) L1.
[7] K. Sreekumar, T.M. Jyothi, T. Mathew, M.B. Talawar, S. Sugunan and B.S. Rao, J. Mol. Catal. A 159 (2000) 327.
[8] K. Nishamol, K.S. Rahna and S. Sugunan, J. Mol. Catal. A 209 (2004) 89.
[9] M.Á. Aramandía, V. Borau, C. Jiménez, J.M. Marinas and F.J. Romero, Appl. Catal. A 183 (1999) 73.
[10] N. Nagaraju and G. Kuriakose, New J. Chem. 27 (2003) 765.
[11] B. Satyavathi, A.N. Patwari and M.B. Rao, Appl. Catal. A 246 (2003) 151.
[12] S. Na rayanan, V.D. Kumari and A.S. Rao, Appl. Catal. A 111 (1994) 133.
[13] T. Esakkidurai and K. Pitchumani, J. Mol. Catal. 218 (2004) 197.
[14] K. Tanabe, M. Misono, Y. Ono and H. Hattori, *New Solid Acids and Bases* (Elsevier, Tokyo, 1989).
[15] K. Tanabe, Catal. Today 78 (2003) 65.
[16] K. Tanabe, Mater. Chem. Phys. 17 (1987) 217.
[17] F.A. Chernyshkova, Russ. Chem. Rev. 62 (1993) 743.
[18] K. Tanabe and S. Okazaki, Appl. Catal. A 133 (1995) 191.
[19] C. Guo and Z. Qian, Catal. Today 16 (1993) 379.
[20] S. Okazaki, M. Kurimata, T. Iizuka and K. Tanabe, Bull. Chem. Soc. Jpn. 60 (1987) 37.
[21] A. Kurosaki, T. Okuyama and S. Okazaki, Bull. Chem. Soc. Jpn. 60 (1987) 3541.
[22] S. Okazaki and N. Wada, Catal. Today 16 (1993) 349.
[23] N. Takamiya, Y. Koinuma, K. Ando and S. Murai, *Nippon Kagakukaishi* (1979) 1452 in [15].
[24] I.I. Ivanova, E.B. Pomakhina, A.I. Rebrov, M. Hunger, Y.G. Kolyagin and J. Weitkamp, J. Catal. 203 (2001) 375.
[25] S.I. Woo, J.K. Lee, B.S. Hong, Y.K. Park and Y.S. Uh, Stud. Surf. Sci. Catal. 49 (1989) 1095.
[26] Y.K. Park, K.U. Park and S.I. Woo, Catal. Lett. 26 (1994) 169.
[27] Patent: Deutsche Offenlegungsschrift 3942413, 21.06.1991 (O. Immel, H. Waldmann, R. Braden).
[28] G.H. Aylward and T.J.V. Findlay, *Datensammlung Chemie in SI-Einheiten* (Wiley-VCH, Weinheim, 1999) (in german).
[29] R. Steudel, *Chemie der Nichtmetalle* (W. de Gruyter, Berlin, 1998) (in german).